

Developmental Plasticity-inspired Adaptive Pruning for Deep Spiking and Artificial Neural Networks

Bing Han^{1,4,#}, Feifei Zhao^{1,#}, Yi Zeng^{1,2,3,4,5,*}, Guobin Shen^{1,5}

¹Research Center for Brain-inspired Intelligence, Institute of Automation,
Chinese Academy of Sciences, Beijing, China

²National Laboratory of Pattern Recognition, Institute of Automation,
Chinese Academy of Sciences, Beijing, China

³Center for Excellence in Brain Science and Intelligence Technology,
Chinese Academy of Sciences, Shanghai, China

⁴School of Artificial Intelligence, University of Chinese Academy of Sciences, Beijing, China

⁵School of Future Technology, University of Chinese Academy of Sciences, Beijing, China

*Corresponding authors: yi.zeng@ia.ac.cn

#Co-first authors with equal contribution

November 24, 2022

Abstract

Developmental plasticity plays a vital role in shaping the brain’s structure during ongoing learning in response to the dynamically changing environments. However, the existing network compression methods for deep artificial neural networks (ANNs) and spiking neural networks (SNNs) draw little inspiration from the brain’s developmental plasticity mechanisms, thus limiting their ability to learn efficiently, rapidly, and accurately. This paper proposed a developmental plasticity-inspired adaptive pruning (DPAP) method, with inspiration from the adaptive developmental pruning of dendritic spines, synapses, and neurons according to the “use it or lose it, gradually decay” principle. The proposed DPAP model considers multiple biologically realistic mechanisms (such as dendritic spine dynamic plasticity, activity-dependent neural spiking trace, local synaptic plasticity), with the addition of an adaptive pruning strategy, so that the network structure can be dynamically optimized during learning without any pre-training and retraining. We demonstrated that the proposed DPAP method applied to deep ANNs and SNNs could learn efficient network architectures that retain only relevant important connections and neurons. Extensive comparative experiments show consistent and remarkable performance and speed boost with the extremely compressed networks on a diverse set of benchmark tasks, especially neuromorphic datasets for SNNs. This work explores how developmental plasticity enables the complex deep networks to gradually evolve into brain-like efficient and compact structures, eventually achieving state-of-the-art (SOTA) performance for biologically realistic SNNs.

Keywords

Developmental Plasticity-inspired Adaptive Pruning, Dendritic Spine Dynamic Plasticity, Improve Learning Speed and Accuracy, Deep ANNs and SNNs Compression

1 Introduction

The human brain with highly plastic is the product of hundreds of millions of years of evolution, thereby allowing infants to emerge with high-level intelligence as they grow and develop. Neural circuits and network topology of the brain are also the products of development over an individual’s life span. Since the birth of the baby, synapses first undergo explosive growth, peaking by age two or three. Then those surplus synapses are gradually eliminated throughout childhood and adolescence according to adaptive pruning mechanisms[1, 2]. This developmental process dynamically shapes the network structure as a result of continuous interaction with the environment and neural changes induced by learning[3, 4]. The developmental plasticity of the brain enables it to show remarkable plasticity in response to the changing environments and to perform multiple complex cognitive functions with extremely low energy consumption. However, current deep neural networks (DNNs) and deep spiking neural networks (DSNNs) employ complex networks with a large number of parameters to solve a single task, which leads to prohibitively expensive computational costs and storage overhead. Besides, DANNs and DSNNs without developmental structural plasticity lack sufficient adaptability and flexibility in learning different tasks. This is a significant gap from baby-like highly-efficient learning and adaptive development.

Taking inspiration from the multi-scale developmental plasticity in the brain, whereby dendritic spines, synapses, and neurons adaptive formation and elimination according to the "use it or lose it" principle, we proposed a developmental plasticity-inspired adaptive pruning (DPAP) method. Incorporating DPAP into the ongoing learning and optimization of neural networks enables DNNs to dynamically prune redundant synapses and neurons according to their activity levels. Different from the existing network compression models, DPAP is remarkable at multiple levels, more biologically plausible with ongoing developmental plasticity, more adaptive pruning for efficient structure shaping, and naturally brings superior performance and learning speed.

The existing model compression methods are intended to reduce the memory and operations consumption while minimizing accuracy drop. The DNNs compression methods include pruning[5], quantization[6, 7]and knowledge distillation[8]. Here, we focus on the pruning methods. DNNs pruning methods considered weight magnitude[9],weight gradient[10, 11], weight similarity[12], Batch Normalization (BN) factor[13] as evaluation criteria, pruning fine-grained individual parameters[14] or coarse-grained overall structures[15, 16]. Deep networks are very sensitive to such pruning strategies, thus pre-training and retraining are required to guarantee performance, which is not biologically plausible. Some developmental plasticity-inspired pruning methods prune neurons or synapses adaptively through a biologically reasonable dynamic strategy, helping to effectively prevent overfitting and underfitting[17, 18, 19]. Such methods are only suitable for shallow artificial neural networks (ANNs), and the pure biological brain development mechanism has not been well understood and referenced.

Spiking Neural Networks (SNNs) are considered to be the third generation neural networks[20], with spike event-driven computation, spatio-temporal information joint processing and high biological plausibility[21], which is more in line with the processing mechanism of the brain nervous network. Therefore, learning from the adaptive pruning mechanism of brain development is an effective way to prune SNNs, which is also lacking in current studies. Many existing methods simply apply pruning approaches in ANNs to SNNs[22, 23, 24, 25, 26], which ignore the unique information processing with binary spikes of SNNs, thus limiting the performance of pruned SNNs. Some more biological SNNs pruning methods use spike-timing dependent plasticity (STDP) as an evaluation criterion, dynamically prune synapses with smaller weights or decayed weights in shallow SNNs [27, 28, 29, 30]. Essentially, STDP as a local unsupervised plasticity mechanism is hard to be applied to deep SNNs learning. Besides, STDP-based pruning strategies are still far from the brain’s pruning mechanism.

Although these attempts have become a feasible way of compressing deep networks, they draw

little inspiration from the brain’s development. Substantial efforts are still needed toward studying developmental plasticity-inspired deep networks, as only such biologically interpretable and plausible methods have the potential to approach the highly efficient brain nervous system. This paper aims to incorporate multi-scale developmental plasticity mechanisms into DNNs and DSNNs and answer how much the brain’s adaptive pruning mechanism helps to better shape the network’s structure.

As the brain ongoing learns, neurons dynamically stretch out multiple dendrites for receiving information, and some dendritic spines form synapses through specific connections[31]. Synaptic plasticity between pre-and postsynaptic neurons contributes to the connectivity and efficiency of neural circuits that support learning, memory, and other cognitive abilities[32, 33]. During developmental pruning of the brain, dendritic spines, synapses, and neurons are continuously strengthened or decayed or even dead according to the ”use it or lose it, gradually decay” principle[34]. Dendritic spines formation (or enlargement) and elimination (or shrinkage) depend on the activity of the postsynaptic neuron: repeated inductions of long-term potentiation (LTP) leads to dendritic spines formation (or enlargement), whereas long-term depression (LTD) coupled with the elimination (or shrinkage) of spines[35, 36]. Repeated activation and frequent use after LTP also strengthen neuronal activity levels and synaptic efficacy. All these activity-driven developmental plasticity mechanisms induce adaptive pruning according to synaptic and neuronal efficacy. Specifically, brain pruning principles include: 1) Synapses and neurons that are rarely used are more likely to be eliminated during the pruning process[37]. 2) Unimportant and redundant synapses and neurons are first gradually decayed and eventually pruned away[38]. 3) Dendritic spine elimination precedes synaptic pruning, and synaptic pruning precedes neural death[39, 40].

Here, we propose a pure Developmental Plasticity-inspired Adaptive Pruning (DPAP) model that incorporates dendritic spine dynamic plasticity, local Bienenstock-Cooper-Munros (BCM) [41] synaptic plasticity, and activity-dependent neural spiking trace as the measure of importance. Based on these biological plausible measures of importance, we designed a novel adaptive pruning strategy to dynamically remove redundant synapses and neurons, which helped to reduce network parameters and energy consumption while improving convergence speed and accuracy. More importantly, the proposed brain-inspired pruning method brings state-of-the-art (SOTA) performance with lower energy consumption for DSNNs on multiple spatial and temporal datasets.

2 Results

2.1 Developmental Plasticity-inspired Adaptive Pruning Algorithm.

DPAP adaptively prunes irrelevant synapses and neurons during the ongoing learning process without any pre-training. The approach is schematically depicted in Fig 1, and works as follows. According to the “use it or lose it” principle, the DPAP takes inspiration from multiscale brain pruning mechanisms, including local synaptic plasticity, activity-dependent neural spiking trace, and dendritic spine dynamic plasticity:

(1)Trace-based BCM synaptic plasticity. We employed trace-based BCM synaptic plasticity to measure the importance (or efficacy) of synapses, as BCM can induce LTP or LTD based on the activity of pre- and post-synaptic neurons, which is consistent with the criterion of brain synaptic pruning. Furthermore, the introduction of spiking trace makes the later the neural firing, the stronger the correlation, which is important for distinguishing the activity magnitude of synapses or neurons during the ongoing pruning process. Trace-based BCM is determined by: $BCM_{pre-post} = S_{pre}S_{post} (S_{post} - \theta)$, where S_{pre} and S_{post} denote the spiking traces of pre-synaptic and post-synaptic neurons, respectively. Threshold θ is the average of historical activity of the post-synaptic neuron. Thus, synaptic importance increases when the trace of the pre-synaptic neuron is

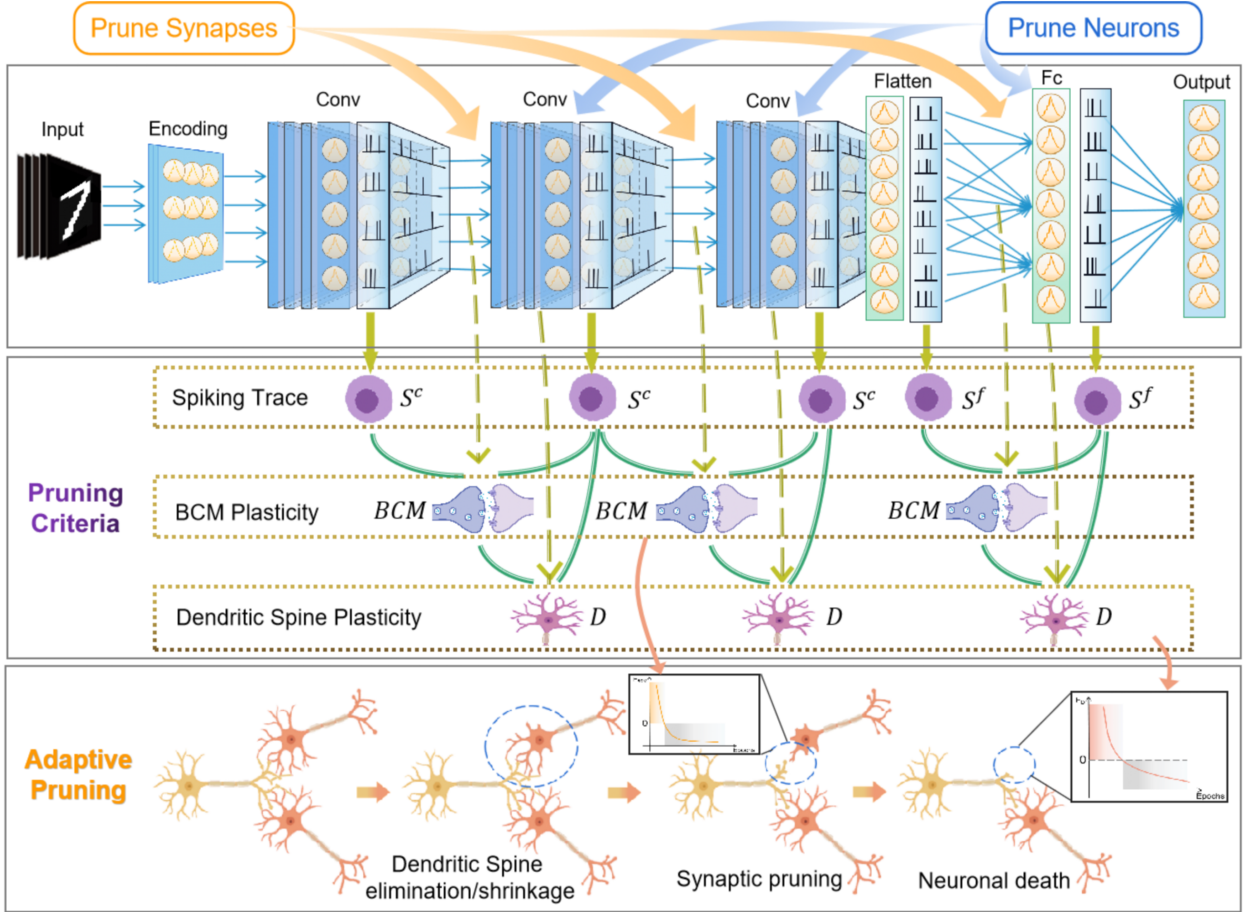


Figure 1: **The procedure of DPAP method.** The SNN structure (**top block**) consists of convolutional layers and fully connected layers. Pruning criteria (**middle block**) contains trace-based BCM plasticity for synapses and dendritic spine plasticity for neurons. Adaptive pruning (**bottom block**) gradually prunes decayed synapses and neurons according to survival function. The orange graph represents the survival function of the pruned synapse, and the red graph represents the survival function of pruned neurons.

sufficient to activate the post-synaptic neurons' trace above a threshold. Otherwise, the synaptic importance declines.

(2) Activity-dependent Neural Spiking Trace. The activity level of the neuron is measured by the spiking trace, which takes into account the spike train in the previous period and the firing state at the current moment. At any time, the neural spiking trace S is accumulated by 1 when the neuron emits a spike, otherwise the trace gradually decays with a time constant τ .

(3) Dendritic Spine Dynamic Plasticity. Neurons extend a large number of dendritic spines to receive presynaptic information, and the density and volume of dendritic spines could reflect the activity level of neurons. For dendritic spines, some spines form synapses with presynaptic axon terminals to receive presynaptic spike signal transmission, and other spines are also expanding and shrinking in preparation for the formation of synaptic connections. Thus, the dynamic plasticity of dendritic spines incorporates the BCM synaptic plasticity with the neural spiking traces. Dendritic spines provide a comprehensive measure of the efficacy and importance of the neurons.

Adaptive Pruning Strategy. DPAP dynamically prunes neurons and synapses in the network on demand. Drawing on the “gradually decay or even die” mechanism in brain developmental pruning, we define a survival function to decide whether synapses or neurons are removed. The survival function takes into account continuous changes in the importance of neurons and synapses, and only neurons and synapses with negative values of the survival function are permanently deleted.

Thus, DPAP could ensure that the pruned synapses and neurons are redundant and unimportant, and naturally more biologically plausible.

DPAP is introduced into DSNNs and DNNs including both convolutional layers and fully connected layers, respectively. For convolutional layers, we adopt structured pruning that treated each channel as an overall neuron population to prune. DSNNs based on leaky integrate-and-fire (LIF) neurons[42] is trained by the surrogate gradient method[43]. DNNs adopt rectified linear unit (ReLU) activation functions and Back propagation training algorithm. Different from DSNNs, DNNs did not have temporal features and spike outputs. Thus, we regarded the float outputs of the artificial neurons as their neural spiking trace.

To verify the effectiveness of the DPAP method, we tested the accuracy, convergence speed and energy consumption of the DPAP on several benchmark tasks, including temporal datasets (N-MNIST[44], DVS-Gesture[45]) and spatial datasets (MNIST[46], CIFAR-10 [47]) for SNNs and spatial datasets (MNIST[46], CIFAR-10 [47]) for DNNs. The convergence speed is defined by minimum epochs required to reach baseline accuracy of the initial network. The energy consumption is defined by the total number of parameters retained after pruning the network. Extensive experiments demonstrated that the DPAP method could remarkably reduced energy consumption while improving convergence speed and accuracy for both DSNNs and DNNs. These results suggest that brain developmental plasticity-inspired adaptive pruning strategy enables the complex deep networks to gradually evolve into brain-like efficient and compact structures, while learning different tasks more accurately and quickly.

2.2 DPAP reduces energy consumption, improves the performance, and speeds up the convergence rate of DSNNs.

We conducted the experiments on four learning tasks to illustrate the superiority of our proposed model: (1) Static Spatial MNIST Dataset: 0-9 ten classes of handwritten digits, dividing into 60 000 training and 10 000 testing samples. Initial DSNNs structure: Input-15C3-AvgPool2-40C3-AvgPool2-Flatten-300FC-10FC. (2) Temporal Neuromorphic N-MNIST Dataset: captured by the neuromorphic vision sensor from original MNIST. Initial DSNNs structure: Input-15C3-AvgPool2-40C3-AvgPool2-Flatten-300FC-10FC. (3) Temporal Neuromorphic DVS-Gesture dataset: 11 different gestures of 29 subjects captured by the DVS camera, with 1176 training samples and 280 testing samples. Initial DSNNs structure: Input-15C3-AvgPool2-40C3-AvgPool2-Flatten-300FC-10FC. (4) CIFAR-10 Dataset: 10 classes of RGB natural images (such as cars, airplanes, ships, etc), dividing into 50,000 training samples and 10,000 testing samples. Initial DSNNs structure: Input-128C3-BN-128C3-BN-MaxPool2-256C3-BN-256C3-BN-MaxPool2-512C3-BN-512C3-BN-Flatten-512FC-10FC.

We first tested the effects of introducing DPAP on the accuracy(Fig. 2A), convergence speed(Fig. 2B) and energy consumption(Fig. 2C) of SNNs for three benchmark datasets: MNIST, N-MNIST, DVS-Gesture. From Fig. 2A and Fig. 2C, we found that introducing DPAP could slightly improve the accuracy (averaged by $\sim 0.31\%$) compared to the initial network without DPAP, while the networks are extremely compressed (averaged by $\sim 63\%$). Compared to the initial network without DPAP, the pruned network with DPAP helped to elevate the test accuracy from 99.46% to 99.59% with only 38.75% energy consumption for MNIST, and from 99.53% to 99.59% with 36.05% energy consumption for N-MNIST, and from 97.83% to 98.56% with 35.97% energy consumption for DVS-Gesture, respectively. These results also highlighted the superiority of our DPAP method on the temporal neuromorphic datasets (such as DVD-Gesture). Besides, the convergence speeds of DSNNs using DPAP are significantly faster (speeds up by $\sim 1.5\times$ as shown in Fig. 2B) than that without DPAP. Especially on N-MNIST dataset, DPAP achieves more outstanding advantages in accelerating convergence (speeds up by $\sim 1.85\times$). In summary, DPAP could elevate the efficiency of DSNNs by extremely compressing network (up to 64%) and speeds up learning (up to $1.85\times$)

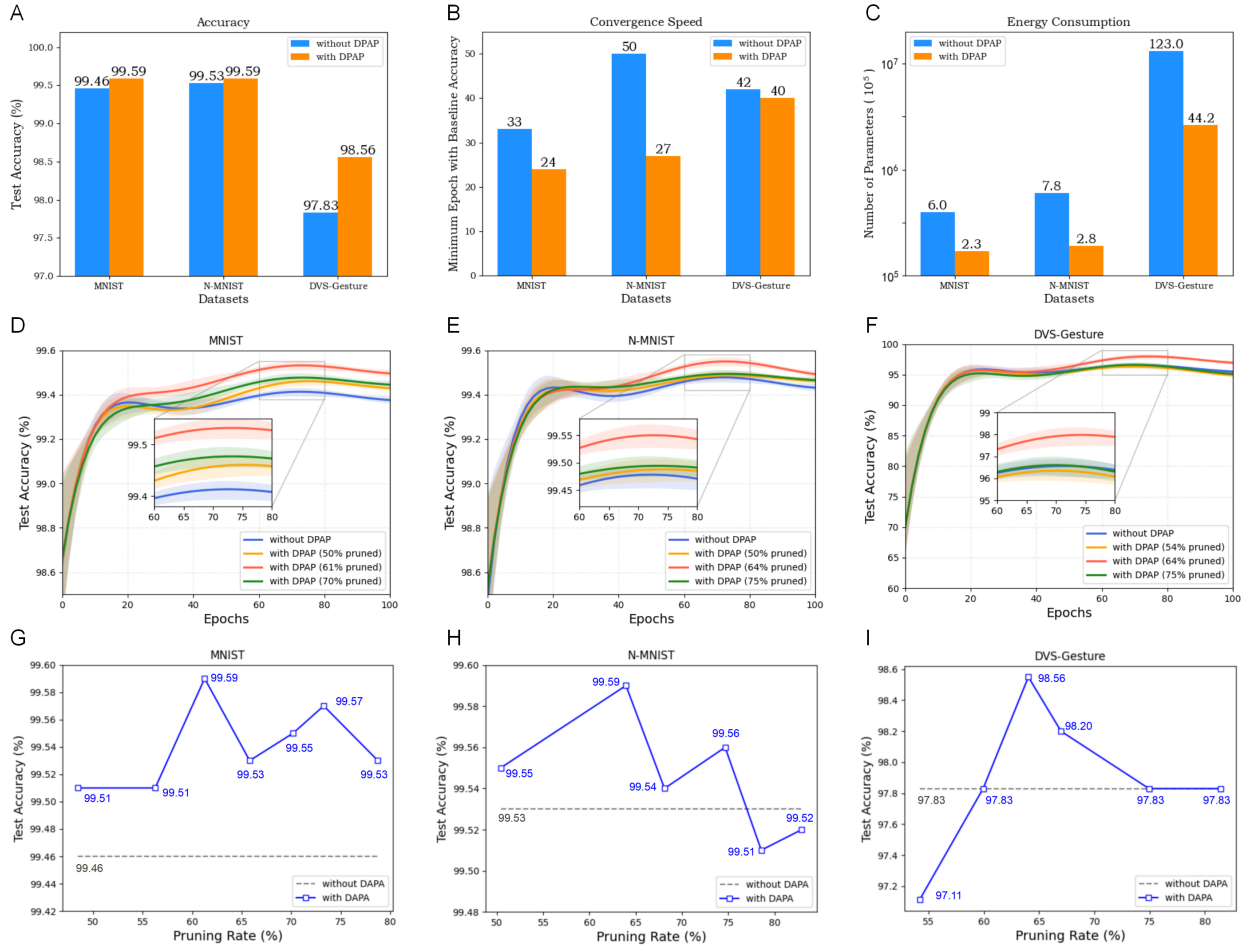


Figure 2: **The effectiveness of introducing DPAP to DSNNs.** The test accuracy (A), convergence speed (B), and energy consumption (C) with and without DPAP for three datasets: MNIST, N-MNIST and DVS-Gesture. (D) to (F): Under different pruning rates, the accuracy changes with the iteration process for different datasets. (G) to (I): The test accuracy achieved by DPAP with different pruning rates for different datasets.

with even relative accuracy improvement (up to 0.73%).

Furthermore, we compared the test accuracy of different datasets during learning by DPAP under different pruning rates and without DPAP (Fig. 2D-F after polynomial fit). Here, the different pruning rates are affected by two parameters (decay value ϵ and decay rate η) of survival function in DPAP method, where the faster neurons and synapses decay, the greater the pruning rate of the final network. Similar conclusions can be obtained with different datasets and pruning rates, that is, DPAP starts to make sense between 20-40 epochs, and then gradually widens the performance gap with the network without DPAP, and eventually achieves the highest performance between 60-80 epochs. Moreover, DPAP could achieve comparable or even better performance under different pruning rates, especially for the MNIST and N-MNIST datasets, which show more adaptable and stable to different pruning rates (Fig. 2D-I).

Fig. 2G-I illustrates the best performance achieved by DPAP with different pruning rates for different datasets. Unlike the conclusion found in most other works that the higher the pruning rate, the worse the performance, we observed that the accuracy peaks at about 60% pruning ratio. Actually, at age two or three, a child’s brain has up to twice as many synapses as it will have in adulthood[2]. Synaptic pruning happens very quickly between ages 2 and 10[48]. During this time, about 50 percent of the extra synapses are eliminated[49]. Subsequently, synaptic pruning continues through adolescence, but not as fast as before. The total number of synapses begins to stabilize[2]. In addition, “over-pruned” or “under-pruned” during brain development would lead to the occurrence

of diseases, such as schizophrenia and autism spectrum disorders, respectively[50, 51, 52]. All these evidence reveal that our conclusions are more biologically reasonable, and closer to the pruning mechanism of brain development.

2.3 Comparison with existing state-of-the-art SNNs compression algorithms for four benchmark datasets.

Table. 1 shows the comparison of the performance of different methods on MNIST, N-MNIST, DVS-Gesture and CIFAR-10 dataset. For the MNIST dataset, other pruning methods compress the network at the cost of an accuracy drop. The ADMM-based pruning method[23] loses 2.23% accuracy when the network is compressed by 75%. Our method could maintain slight performance improvement at different pruning rates ranging from 48.42% to 84.22%. Especially when the pruning rate reaches 84.22%, our method can still achieve an accuracy improvement of 0.1% (accuracy is up to 99.56%). For the N-MNIST dataset, accuracy drops when compressing the network by Grad R[22] and ADMM-based[23] pruning method, such as the accuracy reduces by 2.12% when the network is compressed by 75% for ADMM-based method[23]. Our DPAP method achieves 74.66% compression with even 0.03% relative accuracy improvement, and reaches the maximum accuracy of 99.59 % with 63.95 % pruning rate. For the DVS-Gesture dataset, the accuracy is very sensitive to Deep R[22] pruning method, with 2.53% accuracy drops at 50% pruning rate, and with 2.89% accuracy drops at 75% pruning rate. Our DPAP could still improve the accuracy by 0.73% while compressing the network up to 64.03%. Moreover, even with only 18.55% connections, the accuracy of our method is still up to 97.83% (without any accuracy drop). For the complex CIFAR-10 dataset, our DPAP method achieves 93.83% accuracy at 50.8% pruning rate (with 0.71% accuracy drop). Although there is a slight drop in accuracy, our method still achieves the highest accuracy of 94.27% at the pruning rate of 33.46%, outperforming the highest accuracy of 92.54% with Gard [22] and the highest accuracy of 89.75% with ADMM-based[23] methods. To sum up, compared to other existing state-of-the-art SNNs compression algorithms, our pruning method shows obvious advantages, it can guarantee stable performance improvement under different pruning rates, and achieves SOTA effects on both performance and energy consumption for several benchmark datasets.

2.4 DPAP reduces energy consumption, improves the performance, and speeds up the convergence rate of DNNs.

To verify the generality of our developmental plasticity-inspired pruning model, we also examined the effects of introducing DPAP to DNNs on two classification tasks (MNIST and CIFAR-10). The initial network structure for learning MNIST is: Input-20C5-MaxPool2-50C5-MaxPool2-Flatten-500FC-10FC, for CIFAR-10 is VGG16 network and added BN layers to optimize the weights. Fig.3A-C illustrates the accuracy, convergence speed and energy consumption of the network with DPAP and without DPAP. Notably, DPAP could greatly compress the network (56.00% compressed for MNIST, 41.54% compressed for CIFAR-10) while relatively improving accuracy (0.04% for MNIST, 0.23% for CIFAR-10). In terms of convergence speed, for the MNIST dataset, the original network needs 50 epochs to reach the maximum accuracy of 99.2%, while the network with DPAP can achieve the same accuracy at the 39th epoch. The learning speed accelerated by 1.28 \times . Moreover, for the CIFAR-10 dataset, DPAP improves the convergence speed more than that without DPAP by 2.84 \times . Furthermore, we compared the curve of test accuracy with different pruning rates achieved by DPAP or without DPAP and found that DPAP can consistently improve the performance of the network (Fig.3D,G after polynomial fit). Especially from 100-250 epochs, the accuracy of DNN with DPAP is significantly higher than the baseline DNN without DPAP.

With the datasets of MNIST and CIFAR-10, we also analyzed the accuracy of DNNs with DPAP

Table 1: Performance Comparison of different methods on MNIST, N-MNIST, DVS-Gesture and CIFAR-10 datasets.

Pruning Method	Dataset	Training Methods	Structure	Pruning Rate	Accuracy	Accuracy Loss
Online APTN [53]	MNIST	STDP	2 FC	90.00%	86.53%	-3.87%
Threshold-based [28]	MNIST	STDP	1 FC	70.00%	75.00%	-19.05%
Threshold-based [27]	MNIST	STDP	2 layers	92.00%	91.50%	-1.70%
Threshold-based [54]	MNIST	Event-driven CD	2 FC	74.00%	95.00%	-0.60%
ADMM-based [23]	MNIST	Surrogate Gradient	LeNet-5	50.00%	99.10%	0.03%
				60.00%	98.64%	-0.43%
				75.00%	96.84%	-2.23%
	N-MNIST	Surrogate Gradient	LeNet-5	50.00%	98.34%	-0.61%
				75.00%	96.83%	-2.12%
	CIFAR-10	Surrogate Gradient	7 Conv 2 FC	40.00%	89.75%	0.18%
60.00%				88.35%	-1.18%	
Deep R [22]	MNIST	Surrogate Gradient	2 FC	62.86%	98.56%	-0.36%
				86.70%	98.36%	-0.56%
DVS-Gesture	Surrogate Gradient	2 Conv 2 FC	50.00%	81.59%	-2.53%	
			75.00%	81.23%	-2.89%	
Grad R [22]	MNIST	Surrogate Gradient	2 FC	74.29%	98.59%	-0.33%
				82.06%	98.49%	-0.43%
	N-MNIST	Surrogate Gradient	2 Conv 2 FC	65.00%	99.37%	0.54%
				75.00%	98.56%	-0.27%
	DVS-Gesture	Surrogate Gradient	2 Conv 2 FC	50.00%	84.12%	0.00%
				75.00%	91.95%	7.83%
CIFAR-10	Surrogate Gradient	6 Conv 2 FC	71.59%	92.54%	-0.30%	
			87.96%	92.50%	-0.34%	
DynSNN [55]	MNIST	Surrogate Gradient	3FC	57.40%	99.23%	-0.02%
		ANN-to-SNN	LeNet-5	69.70%	98.98%	-0.27%
	CIFAR-10	ANN-to-SNN	ResNet-20	37.13%	91.13%	-0.23%
		ANN-to-SNN	ResNet-20	37.13%	91.13%	-0.23%
This work	MNIST	Surrogate Gradient	2 Conv 2 FC	48.42%	99.51%	0.05%
				61.25%	99.59%	0.13%
				84.22%	99.56%	0.10%
	N-MNIST	Surrogate Gradient	2 Conv 2 FC	50.41%	99.55%	0.02%
				63.95%	99.59%	0.06%
				74.66%	99.56%	0.03%
	DVS-Gesture	Surrogate Gradient	2 Conv 2 FC	64.03%	98.56%	0.73%
				66.98%	98.20%	0.37%
				81.45%	97.83%	0.00%
				81.45%	97.83%	0.00%
CIFAR-10	Surrogate Gradient	6 Conv 2 FC	33.46%	94.27%	-0.27%	
			39.91%	94.14%	-0.40%	
			50.80%	93.83%	-0.71%	

under different pruning rates, as shown in Fig.3E,H. The results obtained a similar conclusion to DSNNs with DPAP, that as the pruning rate gradually increased, the accuracy showed a trend of increasing first and then decreasing, and formed a clear peak. Specifically, for the MNIST dataset, DNNs with DPAP reached the optimal balance of accuracy at 56.00% pruning rate. Besides, the accuracy consistently exceeds baseline levels from 44.00% to 67.17% of the pruning rate. Even with 67.17% pruning, DPAP can still achieve 99.21% accuracy (improved by 0.01%). For the CIFAR-

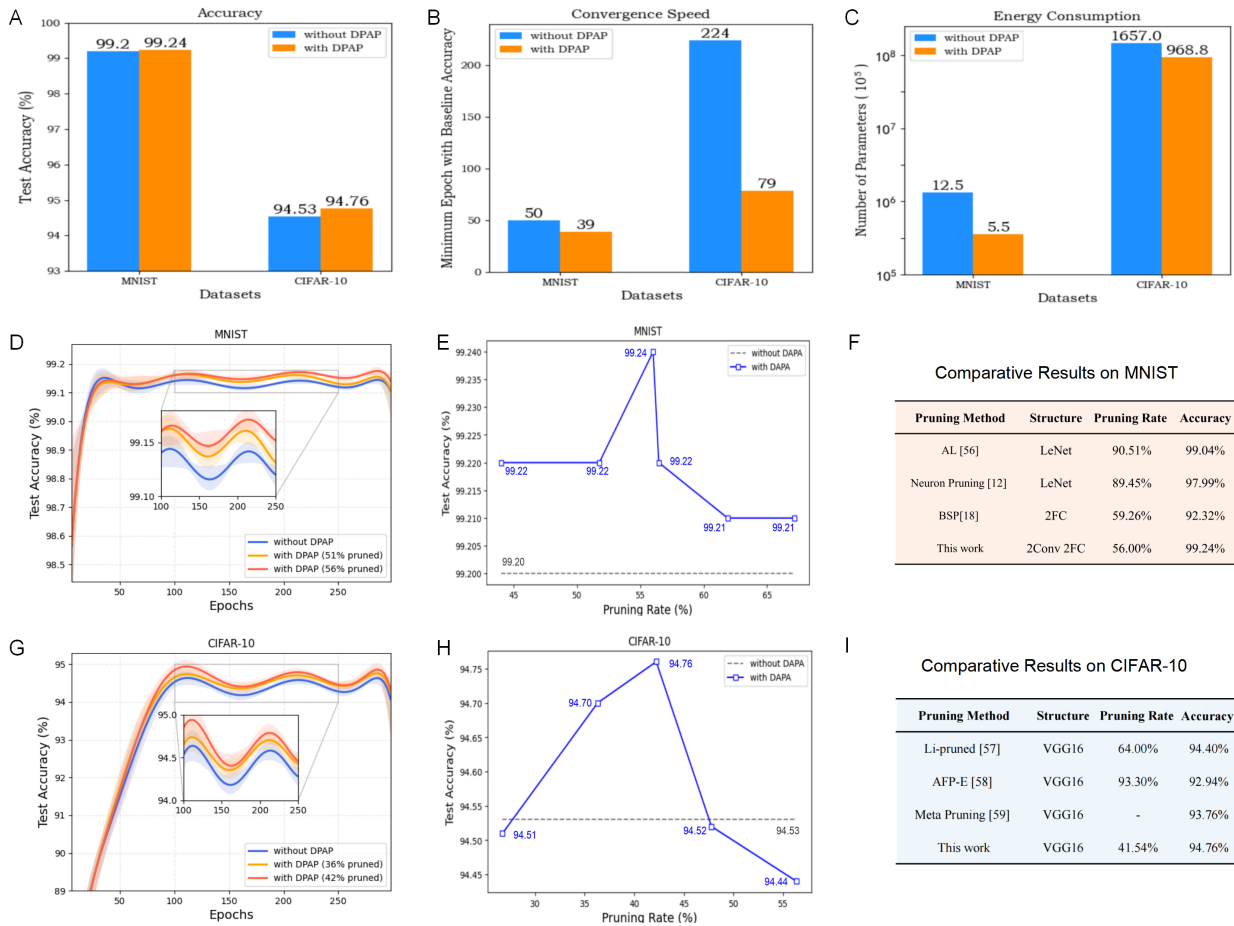


Figure 3: **The effectiveness of introducing DPAP to DNNs.** The test accuracy (A), convergence speed (B), and energy consumption (C) with and without DPAP for MNIST and CIFAR-10 datasets. Under different pruning rates, the accuracy changes with the iteration process for MNIST (D) and CIFAR-10 (G) datasets. Performance comparison between our method and previous work on MNIST (F) [56, 12, 18] and CIFAR-10 (I) [57, 58, 59].

10 dataset, DPAP can improve the accuracy of the network in the case of 36.31% and 41.54% compression, and achieves the highest performance of 94.76% at 41.54% of pruning rate, while the performance is slightly lower (averaged by $\sim 0.04\%$) than the baseline at 26.71%, 47.78%, and 56.37% pruning rate (maintained an acceptable accuracy). In the results mentioned above, the introduction of DPAP to DNNs can achieve optimal effects when the pruning rate is about 48.77% (56.00% for MNIST, 41.54% for CIFAR-10), which is consistent with the biological developmental mechanism. Furthermore, compared to other DNNs pruning algorithms under the same structure, our method achieves comparable performance and accelerates convergence speed. These results also illustrate the effectiveness of introducing the proposed brain development-inspired pruning approach (DPAP) to DNNs.

In conclusion, introducing DPAP into DSNNs and DNNs could effectively improve the accuracy and learning speeds, and extremely compress the networks, showing its general effectiveness, high efficiency and flexible adaptability in various learning tasks and different network structure. More importantly, DPAP, as a brain developmental plasticity-inspired pruning approach, could reveal the brain developmental principle to a certain extent and reflect some characteristics during child development.

3 Discussion

In this study, we introduced biological plausible developmental pruning mechanisms into DNNs and SNNs and demonstrated that the proposed model could help optimize and compress efficient network architectures while improving performance and convergence speed for multiple benchmark datasets. Our DPAP method fully considered multi-scale activity-dependent plasticity, including dendritic spines, synapses, and neurons, as the measure of importance, and employed a brain-like adaptive pruning strategy to gradually eliminate redundant synapses and neurons. To our best knowledge, this is the first work that studies a purely developmental plasticity-inspired pruning model that brings superior performance while also revealing the naturally occurring pruning processes during brain development.

Some conventional methods used to prune DNNs aim to minimize the difference with the pre-trained network as much as possible, such as minimizing reconstruction error[60] or minimizing performance loss[61]. Other pruning DNNs methods use weight magnitude[9], similarity[12], error gradient[11], BN scaling factor[13] as the measures of importance, and prune the most unimportant parameters or channels of the network. However, pruning small weights is unreasonable since small weights can be necessary to maintain accuracy. Existing SNNs pruning methods usually directly apply the pruning method of DNNs to SNNs[23, 24, 25]. These methods do not draw inspiration from the developmental pruning of biological brains, especially for pruning biological SNNs.

In our work, the proposed adaptive pruning strategy is consistent with the developmental pruning mechanism of the brain from multiple perspectives:

(1) Biologically plausible pruning criteria. DPAP method employs local trace-based BCM synaptic plasticity as the measure of synaptic importance. Dendritic spine dynamic plasticity incorporates neuronal activity traces and trace-based BCM synaptic plasticity is used to assess the importance of neurons. Such evaluation criteria are in line with the "activity-dependent, use it or lose it" developmental principle. Based on these pruning criteria, rarely used and unimportant synapses and neurons are pruned during learning. Fig. 4B,D shows the average importance of all neurons and synapses throughout the learning process. We found that after pruning, the retained neurons (Fig. 4A) and synapses (Fig. 4C) are more important, while relatively unimportant ones were eliminated.

(2) Biologically plausible gradual decay or even death. DPAP prunes synapses or neurons is not an instantaneous impulsive decision, but a continuous and thoughtful evaluation. Pruning occurs after several successive gradual decays, where the survival functions for neurons (Fig. 4E) and synapses (Fig. 4F) gradually decline over a period of time before being pruned, which ensures that the pruned synapses or neurons are redundant. This is also consistent with the biological development that dendritic spine enlargement precedes growth, contraction precedes elimination, and synaptic decay precedes elimination[38].

(3) Biologically plausible dynamic pruning. In the brain, pruning is an ongoing process that occurs concurrently with learning[62]. The pruning process is not arbitrary, but first drops sharply, then slowly decreases, and finally tends to be stable[2]. Specifically, dendritic spine elimination precedes synaptic pruning, and synaptic pruning precedes neural death[39, 40]. We examined whether the DPAP model can represent these dynamic phenomena in brain developmental pruning. Results are as expected the total number of connections in the network falls sharply at first and then gradually keeps steady during learning (see Fig. 4G). Furthermore, the average number of synapses contained in pruned neurons is 272, while in retained neurons is 298, which indicates that neurons with more pruned synapses are more likely to be deleted. Moreover, the shrinkage and elimination of dendritic spines result from the reduction of neuronal activity and synaptic plasticity, which also leads to the deletion of synapses. Therefore, we can conclude that the shrinkage and elimination of dendritic spines and synaptic pruning are prerequisites for neuronal pruning.

A small number of brain-like SNNs pruning methods dynamically prune synapses with smaller

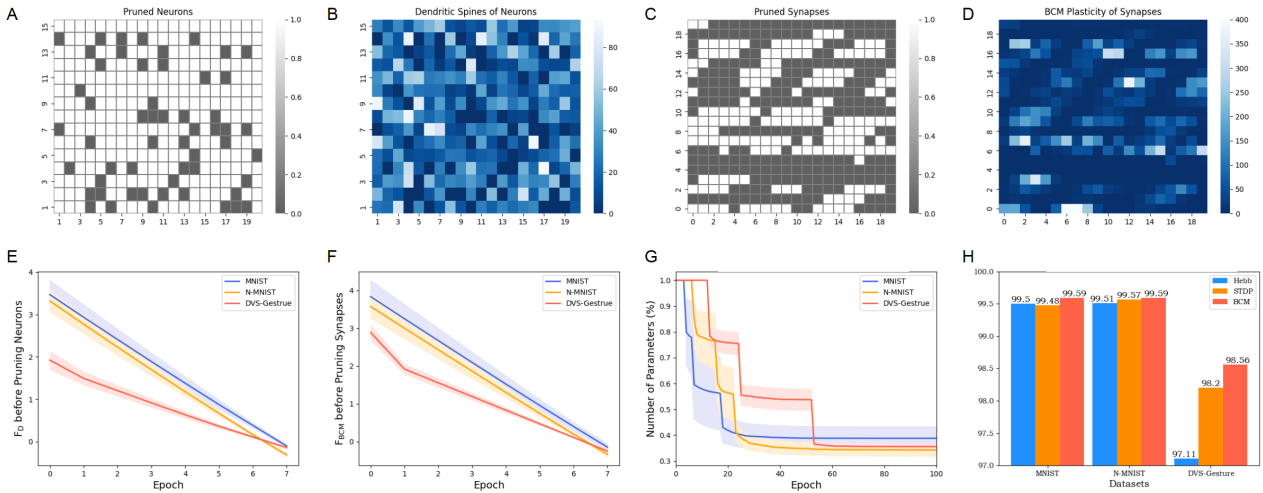


Figure 4: Analyses of the biological plausibility of DPAP. The retained neurons **(A)** (or synapses **(C)**) and the average importance of all neurons **(B)** (or synapses **(D)**) in the first fully connected layer of DSNNs for MNIST dataset. The white squares represent pruned neurons and synapses. **E** and **F**: During the 8 epochs before the neurons or synapses are pruned, the changing of survival function F_D and F_{BCM} for MNIST, N-MNIST, and DVS-Gesture datasets. **G**: The changing of network parameters during learning with DPAP. **(H)**: Test accuracy comparison of different synaptic plasticity used in DPAP for different datasets.

weights or decayed weights in shallow SNNs based on the STDP measure of importance[27, 28, 29, 30]. Although STDP is a feasible and biological realistic measure of importance, that depends on the spike timing difference of the pre-synaptic and post-synaptic neurons[63, 64, 65], it is not entirely consistent with the biological LTP and LTD. Unlike STDP and Hebbian[32] synaptic modification, BCM theory accounts for experience-dependent synaptic plasticity that could undergo both LTP or LTD depending on the level of postsynaptic response[66, 41]. There is substantial evidence both in the hippocampus and visual cortex that active synapses undergo LTD or LTP depending on the level of postsynaptic spiking which is consistent with the BCM theory[67, 68, 69, 70, 71]. To illustrating the superiority of BCM plasticity, we conducted the experiments on SNNs pruning with BCM, STDP, and Hebb plasticity, respectively. As shown in Fig. 4H, replacing BCM with Hebb and STDP will reduce the test accuracy for different datasets, while the more brain-like BCM used in our method achieves the best results.

Taken together, we demonstrated that introducing a novel developmental pruning strategy helped to adaptively compress and optimize the network during the ongoing learning through pruning away redundant synapses and neurons. In contrast to existing pruning methods, our model incorporated multi-scale developmental plasticity that led to a more compact and efficient network while improving the performance and convergence speed. The proposed method achieves the SOTA results on different datasets for DSNNs. More importantly, our approach shows highly biological plausible and provides insight into naturally occurring pruning in the developing brain from multiple aspects. Although we demonstrated the effectiveness of brain development-inspired pruning algorithms on DNNs and DSNNs, the DPAP approach should also be applicable to other network architectures, such as reservoir networks that are not hierarchical. In addition, this paper considered the developmental pruning mechanism. we expect the further studies combine developmental growth to realize the gradual evolution from small into a complex but efficient network that could adapt to the dynamic changing environment.

4 Methods

4.1 The Components of SNNs

LIF neuron. This paper adopts LIF neurons[42] with biological plausible characteristics as the basic information processing unit of SNNs. The membrane potential of the LIF neuron is accumulated by dynamically integrating the spikes of the presynaptic neuron during T time windows. When the postsynaptic membrane potential reaches the threshold $V_{th} = 0.5$, the postsynaptic neuron fires and the membrane potential is reset to zero, shown as follows:

$$u_i^{t+1,n} = \lambda u_i^{t,n} (1 - o_i^{t,n}) + \sum_{j=1}^{l(n-1)} w_{ij} o_j^{t+1,n-1} + b_i \quad (1)$$

$$o_i^{t+1,n} = \begin{cases} 1, & u_i^{t+1,n} \geq V_{th} \\ 0, & otherwise \end{cases} \quad (2)$$

where $\lambda = 0.2$ is a time constant, $u_i^{t,n}$ and $o_i^{t,n}$ are the membrane potential and spike of the i -th neuron in n -th layer at time t , respectively. w_{ij} is the synaptic strength from the presynaptic j -th neuron to postsynaptic i -th neuron.

Training procedure. For global training, we define the spiking frequency of neurons in the output layer as the final output of the SNNs. Thus, the mean squared error (MSE) loss function L is calculated as follows:

$$L = \|Y^{label} - \frac{1}{T} \sum_{t=1}^T o^{t,N}\|_2^2 \quad (3)$$

where Y^{label} denotes the real one-hot label, T is the given time window and N is the number of neurons in the last layer. Due to the non-differentiability of spikes, we train the SNNs by surrogate gradient backpropagation [43] which uses the differentiable functions to approximate the derivatives of spike activity. Here, we use the rectangle function to represent the differentiable functions:

$$H(u_i^{t+1,n}) = \frac{1}{a} \text{sign} \left(|u_i^{t+1,n} - V_{th}| < \frac{a}{2} \right) \quad (4)$$

where $a = 1$ is a constant that determines the peak width of the function.

4.2 Biologically Plausible Pruning Criteria for SNNs

Activity-dependent neural spiking trace. The neural spiking trace responds to the activity level of the spiking neurons. At the t -th time step, if the neuron fires, its spiking trace S will be added by 1. Otherwise, its spiking trace decayed with time constant $\tau = 0.5$. For the fully connected layer, the spiking trace of the i -th neuron in n -th layer at time $t+1$ is calculated as follows:

$$S_i^{t+1,f} = \tau S_i^{t,f} + o_i^{t+1,f} \quad (5)$$

Considering the structural characteristics of the convolutional layer, we regard each channel as an entire population of neurons. The neural spiking trace for the convolution layer which has $C \times N \times N$ neurons is calculated as follows:

$$S_i^{t+1,c} = \tau S_i^{t,c} + \sum_{k=1}^{N,N} o_i^{t+1,c} \quad (6)$$

Trace-based BCM synaptic plasticity. The trace-based BCM is measured by a combination of the pre- and post-synaptic neural spiking traces, the difference between the post-synaptic neural spiking traces and the sliding threshold θ . For each batch, the neural spiking trace S is accumulated over the T time window as Eq 5,6, then trace-based BCM of b-th batch is calculated by:

$$BCM_{pre-post}^b = S_{pre}^T \cdot S_{post}^T \cdot (S_{post}^T - \theta) \quad (7)$$

where S_{pre}^T and S_{post}^T are the pre- and post- spiking trace over T time windows, respectively. The sliding threshold θ is the average of history postsynaptic activity, as shown in Eq 8. It determines the direction of LTP and LTD synaptic plasticity based on the activity of postsynaptic neurons.

$$\theta = \frac{\theta * (Num - 1) + S_{post}}{Num} \quad (8)$$

where Num is the number of all the batches experienced from the beginning of learning. At the b-th batch in the e-th epoch, Num is the following value:

$$Num = e * BatchSize + b \quad (9)$$

For each epoch, BCM^e is calculated as the sum of all batches:

$$BCM^e = \sum_{b=1}^{BatchSize} BCM_{pre-post}^b \quad (10)$$

Dendritic spine dynamic plasticity. Dendritic spine plasticity is jointly determined by the neural spiking traces and the trace-based BCM synaptic plasticity. For each epoch, dendritic spine dynamic plasticity is calculated as follows:

$$D^e = \sum_{b=1}^{BatchSize} S_{post}^T * \sum_{j=1}^{N_{pre}} BCM^e \quad (11)$$

where N_{pre} is the number of presynaptic channels or neurons.

4.3 Developmental Plasticity-inspired Adaptive Pruning

DPAP in SNNs. The DPAP method prunes unimportant synapses and neurons according to their importance BCM^e and D^e . Inspired by the pruning mechanism of brain development, we designed the survival function for neuron F_D and synapse F_{BCM} . At the beginning of learning, we initialized the survival functions as a constant β . For each epoch, the trace-based BCM synaptic plasticity for measuring synapses and dendritic spine dynamic plasticity for measuring neurons are linearly normalized:

$$\delta_{BCM}^e = 2 * Normalized(BCM^e) - \epsilon \quad (12)$$

$$\delta_D^e = 2 * Normalized(D^e) - \epsilon \quad (13)$$

where ϵ is the decay value. Then, we calculated the update value of BCM survival function ΔF_{BCM}^e and dendritic spine survival function ΔF_D^e :

$$\Delta F_{BCM}^e = \begin{cases} \delta_{BCM}^e + C, & \delta_{BCM}^e \geq 0 \\ \delta_{BCM}^e, & otherwise \end{cases} \quad (14)$$

$$\Delta F_D^e = \begin{cases} \delta_D^e + C, & \delta_D^e \geq 0 \\ \delta_D^e, & otherwise \end{cases} \quad (15)$$

For the reliability of pruning, we protected neurons or synapses with positive decay value by extra increasing by constant C ($C = 5$ in convolutional layers, $C = 2$ in fully connected layers). During the whole learning process, the survival function F_{BCM} and F_D are updated as the decay rate η :

$$F_{BCM} = \gamma F_{BCM} + e^{-\frac{epoch}{\eta}} \Delta F_{BCM}^e \quad (16)$$

$$F_D = \gamma F_D + e^{-\frac{epoch}{\eta}} \Delta F_D^e \quad (17)$$

where $\gamma = 0.999$ is the decay constant of the survival function. Finally, we prune the synapses whose $F_{BCM} < 0$ by setting their weight $w_{ij} = 0$, prune the neurons whose $F_D < 0$ by setting all their presynaptic weight $W_i = 0$ at each epoch.

DPAP in DNNs. For traditional DNNs, we employed the simple neuron with RELU activation function. The cross-entropy loss function was used to evaluate error, and the standard BP was used to update the network weight. Corresponding to SNNs, the neural spiking trace of the neuron in DNNs was defined as the output of the neurons after activation function. For the fully connected layer

$$S_i^{DNN,f} = RELU \left(W_f x_j^{f-1} + b_f \right) \quad (18)$$

For the convolution layer with $C \times N \times N$ neurons

$$S_i^{DNN,c} = \sum_{k=1}^{N,N} RELU \left(W_c \otimes x_j^{c-1} + b_c \right) \quad (19)$$

where x_j^{f-1} and x_j^{c-1} is the inputs of the layer.

For each batch, the trace-based BCM synaptic plasticity $BCM_{pre-post}^b$ is calculated same as Eq 7 based on pre- and post- spiking trace as Eq 18,19. The sliding threshold is update as Eq 8. For each epoch, the BCM^e is the sum of $BCM_{pre-post}^b$ and the dendritic spine D^e is calculated same as Eq 11. Besides, the adaptive pruning strategy in DNNs is the same as in SNNs as Eq 12 to 17.

The detailed procedure of the DPAP method.

For a feed-forward SNN or DNN, we provide the detailed procedure for the DPAP algorithm as follow:

Initialization: randomly initialize network weight W , initialize $F_{BCM} = \beta$, $F_D = \beta$ for each layer.

For e in *Epoch*:

 For b in *Batch*:

 For t in T :

 Forward propagation getting outputs as Eq 1,2.

 Calculate spiking trace as Eq 5,6 or Eq18,19.

 end

Back propagation by surrogate gradient BP for SNN as Eq 3,4 or standard BP for DNN.
 Calculate $BCM_{pre-post}^b$ as Eq 7,8.
 end
 Calculate BCM^e and D^e as Eq 10 and 11, respectively.
 Calculate the F_{BCM} and F_D as Eq 12 to Eq 17.
 Pruned neurons and synapses whose survival function was less than 0.
 end

Data availability

The data used in this study are available in the following databases.

The MNIST data[46]: <http://yann.lecun.com/exdb/mnist/>.

The N-MNIST data[44]: <https://www.garrickorchard.com/datasets/n-mnist>.

The DVS-GESTURE data[45]: <https://www.research.ibm.com/dvsgesture>.

The CIFAR-10 data[47]: <https://www.cs.toronto.edu/~kriz/cifar.html>.

Acknowledgments

This work is supported by the National Key Research and Development Program (Grant No. 2020AAA0107800), the Strategic Priority Research Program of the Chinese Academy of Sciences (Grant No. XDB32070100), the National Natural Science Foundation of China (Grant No. 62106261), the Key Research Program of Frontier Sciences, Chinese Academy of Sciences (Grant No. ZDBS-LY-JSC013), and Beijing Academy of Artificial Intelligence (BAAI).

References

- [1] Huttenlocher, P. R. *Neural plasticity: The effects of environment on the development of the cerebral cortex* (Harvard University Press, 2009).
- [2] Huttenlocher, P. R. *et al.* Synaptic density in human frontal cortex-developmental changes and effects of aging. *Brain Res* **163**, 195–205 (1979).
- [3] Elman, J. L., Bates, E. A. & Johnson, M. H. *Rethinking innateness: A connectionist perspective on development*, vol. 10 (MIT press, 1996).
- [4] Johnson, M. H. Functional brain development in humans. *Nature Reviews Neuroscience* **2**, 475–483 (2001).
- [5] Han, S., Pool, J., Tran, J. & Dally, W. J. Learning both weights and connections for efficient neural networks. In *Proceedings of the 28th International Conference on Neural Information Processing Systems - Volume 1*, 1135–1143 (MIT Press, 2015).
- [6] Han, S., Mao, H. & Dally, W. J. Deep compression: Compressing deep neural networks with pruning, trained quantization and huffman coding. *Fiber* **56**, 3–7 (2015).
- [7] Hubara, I., Courbariaux, M., Soudry, D., El-Yaniv, R. & Bengio, Y. Quantized neural networks: Training neural networks with low precision weights and activations. *The Journal of Machine Learning Research* **18**, 6869–6898 (2017).
- [8] Hinton, G., Vinyals, O. & Dean, J. Distilling the knowledge in a neural network. *Computer Science* **14**, 38–39 (2015).

- [9] Molchanov, P., Tyree, S., Karras, T., Aila, T. & Kautz, J. Pruning convolutional neural networks for resource efficient inference. *arXiv preprint arXiv:1611.06440* (2016).
- [10] Hassibi, B., Stork, D. G. & Wolff, G. J. Optimal brain surgeon and general network pruning. In *IEEE international conference on neural networks*, 293–299 (IEEE, 1993).
- [11] Huang, Z. & Wang, N. Data-driven sparse structure selection for deep neural networks. In *Proceedings of the European conference on computer vision (ECCV)*, 304–320 (2018).
- [12] Srinivas, S. & Babu, R. V. Data-free parameter pruning for deep neural networks. *arXiv preprint arXiv:1507.06149* (2015).
- [13] You, Z., Yan, K., Ye, J., Ma, M. & Wang, P. Gate decorator: Global filter pruning method for accelerating deep convolutional neural networks. *Advances in neural information processing systems* **32** (2019).
- [14] Yang, M., Faraj, M., Hussein, A. & Gaudet, V. Efficient hardware realization of convolutional neural networks using intra-kernel regular pruning. In *2018 IEEE 48th International Symposium on Multiple-Valued Logic (ISMVL)*, 180–185 (IEEE, 2018).
- [15] Wen, W., Wu, C., Wang, Y., Chen, Y. & Li, H. Learning structured sparsity in deep neural networks. *Advances in neural information processing systems* **29** (2016).
- [16] Yu, F. *et al.* Width & depth pruning for vision transformers. In *AAAI Conference on Artificial Intelligence (AAAI)*, vol. 2022 (2022).
- [17] Zhao, F., Zeng, Y. & Bai, J. Toward a brain-inspired developmental neural network based on dendritic spine dynamics. *Neural Computation* **34**, 172–189 (2022).
- [18] Zhao, F. & Zeng, Y. Dynamically optimizing network structure based on synaptic pruning in the brain. *Frontiers in Systems Neuroscience* **15**, 55 (2021).
- [19] Zhao, F., Zhang, T., Zeng, Y. & Xu, B. Towards a brain-inspired developmental neural network by adaptive synaptic pruning. In *International Conference on Neural Information Processing*, 182–191 (Springer, 2017).
- [20] Maass, W. Networks of spiking neurons: The third generation of neural network models. *Neural networks* **10**, 1659–1671 (1997).
- [21] Gerstner, W. & Kistler, W. M. *Spiking neuron models: Single neurons, populations, plasticity* (Cambridge university press, 2002).
- [22] Chen, Y., Yu, Z., Fang, W., Huang, T. & Tian, Y. Pruning of deep spiking neural networks through gradient rewiring. In *IJCAI* (2021).
- [23] Deng, L. *et al.* Comprehensive snn compression using admm optimization and activity regularization. *IEEE transactions on neural networks and learning systems* 1–15 (2021).
- [24] Wu, D., Lin, X. & Du, P. An adaptive structure learning algorithm for multi-layer spiking neural networks. In *2019 15th International Conference on Computational Intelligence and Security (CIS)*, 98–102 (IEEE, 2019).
- [25] Lee, D., Park, S., Kim, J., Doh, W. & Yoon, S. Energy-efficient knowledge distillation for spiking neural networks. *arXiv preprint arXiv:2106.07172* (2021).

- [26] Kundu, S., Datta, G., Pedram, M. & Beerel, P. A. Spike-thrift: Towards energy-efficient deep spiking neural networks by limiting spiking activity via attention-guided compression. In *2021 IEEE Winter Conference on Applications of Computer Vision (WACV)*, 3952–3961 (IEEE, 2021).
- [27] Rathi, N., Panda, P. & Roy, K. Stdp-based pruning of connections and weight quantization in spiking neural networks for energy-efficient recognition. *IEEE Transactions on Computer-Aided Design of Integrated Circuits and Systems* **38**, 668–677 (2018).
- [28] Shi, Y., Nguyen, L., Oh, S., Liu, X. & Kuzum, D. A soft-pruning method applied during training of spiking neural networks for in-memory computing applications. *Frontiers in neuroscience* **13**, 405 (2019).
- [29] Qi, Y. *et al.* Jointly learning network connections and link weights in spiking neural networks. In *Proceedings of the 27th International Joint Conference on Artificial Intelligence*, 1597–1603 (2018).
- [30] Nguyen, T. N., Veeravalli, B. & Fong, X. Connection pruning for deep spiking neural networks with on-chip learning. In *International Conference on Neuromorphic Systems 2021*, 1–8 (2021).
- [31] Gray, E. G. Axo-somatic and axo-dendritic synapses of the cerebral cortex: an electron microscope study. *Journal of anatomy* **93**, 420 (1959).
- [32] Hebb, D. O. The first stage of perception: growth of the assembly. *The Organization of Behavior* **4**, 60–78 (1949).
- [33] Skaliora, I. Experience-dependent plasticity in the developing brain. In *International Congress Series*, vol. 1241, 313–320 (Elsevier, 2002).
- [34] Bruer, J. T. Neural connections: Some you use, some you lose. *The Phi Delta Kappan* **81**, 264–277 (1999).
- [35] Toni, N., Buchs, P.-A., Nikonenko, I., Bron, C. & Muller, D. Ltp promotes formation of multiple spine synapses between a single axon terminal and a dendrite. *Nature* **402**, 421–425 (1999).
- [36] Becker, N., Wierenga, C. J., Fonseca, R., Bonhoeffer, T. & Nägerl, U. V. Ltp induction causes morphological changes of presynaptic boutons and reduces their contacts with spines. *Neuron* **60**, 590–597 (2008).
- [37] Chugani, H. T. Neuroimaging of developmental nonlinearity and developmental pathologies. *Developmental neuroimaging: Mapping the development of brain and behavior* 187–195 (1996).
- [38] Colman, H., Nabekura, J. & Lichtman, J. Alterations in synaptic strength preceding axon withdrawal. *Science* **275**, 356–361 (1997).
- [39] Trachtenberg, J. T. *et al.* Long-term in vivo imaging of experience-dependent synaptic plasticity in adult cortex. *Nature* **420**, 788–794 (2002).
- [40] Furber, S., Oppenheim, R. W. & Prevette, D. Naturally-occurring neuron death in the ciliary ganglion of the chick embryo following removal of preganglionic input: evidence for the role of afferents in ganglion cell survival. *Journal of Neuroscience* **7**, 1816–1832 (1987).

- [41] Bienenstock, E. L., Cooper, L. N. & Munro, P. W. Theory for the development of neuron selectivity: orientation specificity and binocular interaction in visual cortex. *Journal of Neuroscience* **2**, 32–48 (1982).
- [42] Abbott, L. F. Lapicque’s introduction of the integrate-and-fire model neuron (1907). *Brain Research Bulletin* **50**, 303–304 (1999).
- [43] Wu, Y., Deng, L., Li, G., Zhu, J. & Shi, L. Spatio-temporal backpropagation for training high-performance spiking neural networks. *Frontiers in neuroscience* **12**, 331 (2018).
- [44] Orchard, G., Jayawant, A., Cohen, G. K. & Thakor, N. Converting static image datasets to spiking neuromorphic datasets using saccades. *Frontiers in neuroscience* **9**, 437 (2015).
- [45] Amir, A. *et al.* A low power, fully event-based gesture recognition system. In *Proceedings of the IEEE conference on computer vision and pattern recognition*, 7243–7252 (2017).
- [46] LeCun, Y. The mnist database of handwritten digits. <http://yann.lecun.com/exdb/mnist/> (1998).
- [47] Krizhevsky, A., Hinton, G. *et al.* Learning multiple layers of features from tiny images (2009).
- [48] Huttenlocher, P. R. Synaptogenesis, synapse elimination, and neural plasticity in human cerebral cortex. (1994).
- [49] Huttenlocher, P. R. Morphometric study of human cerebral cortex development. *Neuropsychologia* **28**, 517–527 (1990).
- [50] Penzes, P., Cahill, M. E., Jones, K. A., VanLeeuwen, J.-E. & Woolfrey, K. M. Dendritic spine pathology in neuropsychiatric disorders. *Nature neuroscience* **14**, 285–293 (2011).
- [51] Glausier, J. R. & Lewis, D. A. Dendritic spine pathology in schizophrenia. *Neuroscience* **251**, 90–107 (2013).
- [52] Hutsler, J. J. & Zhang, H. Increased dendritic spine densities on cortical projection neurons in autism spectrum disorders. *Brain research* **1309**, 83–94 (2010).
- [53] Guo, W., Fouda, M. E., Yantir, H. E., Eltawil, A. M. & Salama, K. N. Unsupervised adaptive weight pruning for energy-efficient neuromorphic systems. *Frontiers in Neuroscience* 1189 (2020).
- [54] Neftci, E. O., Pedroni, B. U., Joshi, S., Al-Shedivat, M. & Cauwenberghs, G. Stochastic synapses enable efficient brain-inspired learning machines. *Frontiers in neuroscience* **10**, 241 (2016).
- [55] Liu, F., Zhao, W., Chen, Y., Wang, Z. & Dai, F. Dynsnn: A dynamic approach to reduce redundancy in spiking neural networks. In *ICASSP 2022-2022 IEEE International Conference on Acoustics, Speech and Signal Processing (ICASSP)*, 2130–2134 (IEEE, 2022).
- [56] Srinivas, S. & Babu, R. V. Learning the architecture of deep neural networks. In *Proceedings of the British Machine Vision Conference (BMVC)*, pages, 104–1 (2016).
- [57] Li, H., Kadav, A., Durdanovic, I., Samet, H. & Graf, H. P. Pruning filters for efficient convnets. *arXiv preprint arXiv:1608.08710* (2016).

- [58] Ding, X., Ding, G., Han, J. & Tang, S. Auto-balanced filter pruning for efficient convolutional neural networks. In *Proceedings of the AAAI Conference on Artificial Intelligence*, vol. 32 (2018).
- [59] He, Y., Liu, P., Zhu, L. & Yang, Y. Meta filter pruning to accelerate deep convolutional neural networks. *arXiv preprint arXiv:1904.03961* (2019).
- [60] Luo, J.-H., Wu, J. & Lin, W. Thinet: A filter level pruning method for deep neural network compression. In *Proceedings of the IEEE international conference on computer vision*, 5058–5066 (2017).
- [61] He, Y., Kang, G., Dong, X., Fu, Y. & Yang, Y. Soft filter pruning for accelerating deep convolutional neural networks. In *IJCAI International Joint Conference on Artificial Intelligence* (2018).
- [62] Rakic, P., Bourgeois, J.-P., Eckenhoff, M. F., Zecevic, N. & Goldman-Rakic, P. S. Concurrent overproduction of synapses in diverse regions of the primate cerebral cortex. *Science* **232**, 232–235 (1986).
- [63] Poo, M.-M. Spike timing-dependent plasticity: Hebb’s postulate revisited. *International Journal of Developmental Neuroscience* **26**, 827–828 (2008).
- [64] Bell, C. C., Han, V. Z., Sugawara, Y. & Grant, K. Synaptic plasticity in a cerebellum-like structure depends on temporal order. *Nature* **387**, 278–281 (1997).
- [65] Gerstner, W., Kempter, R., Hemmen, J. L. V. & Wagner, H. A neuronal learning rule for sub-millisecond temporal coding. *Nature* **383**, 76–78 (1996).
- [66] Kirkwood, A., Rioult, M. G. & Bear, M. F. Experience-dependent modification of synaptic plasticity in visual cortex. *Nature* **381**, 526–528 (1996).
- [67] Bear, M. F., Cooper, L. N. & Ebner, F. F. A physiological basis for a theory of synapse modification. *Science* **237**, 42–48 (1987).
- [68] Abraham, W. C., Mason-Parker, S. E., Bear, M. F., Webb, S. & Tate, W. P. Heterosynaptic metaplasticity in the hippocampus in vivo: a bcm-like modifiable threshold for ltp. *Proceedings of the National Academy of Sciences* **98**, 10924–10929 (2001).
- [69] Dudek, S. M. & Bear, M. F. Homosynaptic long-term depression in area ca1 of hippocampus and effects of n-methyl-d-aspartate receptor blockade. *Proceedings of the National Academy of Sciences* **89**, 4363–4367 (1992).
- [70] Kirkwood, A. & Bear, M. F. Homosynaptic long-term depression in the visual cortex. *Journal of Neuroscience* **14**, 3404–3412 (1994).
- [71] Artola, A., Bröcher, S. & Singer, W. Different voltage-dependent thresholds for inducing long-term depression and long-term potentiation in slices of rat visual cortex. *Nature* **347**, 69–72 (1990).

Contributions

B.H.,F.Z. and Y.Z. designed the study. B.H.,F.Z. and G.S.performed the experiments and the analyses. B.H.,F.Z. and Y.Z. wrote the paper.

Competing interests

The authors declare no competing interests.